16th World Conference on Earthquake Engineering, 16WCEE 2017

Santiago Chile, January 9th to 13th 2017

Paper N° 2098 (Abstract ID)

Registration Code: S- J1461961332

DAMPING COEFFICIENT OF A BUILDING WITH BRB SUBJECT TO THREE TYPES OF EARTHQUAKE GROUND MOTIONS

G. Palazzo[(1)], C. Bay[(2)], V. Roldan[(3)], F. Calderon[(4)], M. Guzmán[(5)] and F. López-Almansa[(6)]

[(1)] *Professor, National Technological University, Ceredetec, Argentina, gpalazzo@frm.utn.edu.ar*
[(2)] *Professor, National Technological University, Argentina, cbay@frsr.utn.edu.ar*
[(3)] *Professor Assistant, National Technological University, Ceredetec, Argentina, victor.roldan@frm.utn.edu.ar*
[(4)] *Professor Assistant, National Technological University, Ceredetec, Argentina, francisco.calderon@frm.utn.edu.ar*
[(5)] *Professor, National Technological University, Ceredetec, Argentina, gpalazzo@frm.utn.edu.ar*
[(6)] *Professor, Technical University of Catalonia, Spain, francesc.lopez-almansa@upc.edu*

Abstract

This study evaluates the damping coefficient, the effective damping and the energy dissipated of a structure with and without buckling-restrained braces (BRB), subjected to 30 seismic records with different characteristics. These results are compared with the damping coefficient given by an international standard. The structure was modelled with a commercial software. The study is carried out on a symmetric 4-story steel moment-resisting frame that was tested without BRB at the E-Defense laboratory in Japan. The dynamic response of such unbraced bare frame was numerically simulated, obtaining a satisfactory agreement. The same numerical model was used to describe the dynamic behavior of the steel frame equipped with BRB. The seismic were three types of seismic records: Far-Field (inter and intra plate), and Near-Field (ten ground motion records in each series). These records were considered with and without scaling. Scaling was performed according to one of the Argentinian code`s spectrum. The results of the numerical modeling (damping coefficient, effective damping and energy dissipated) were discussed. In the conclusion, the main results of the study are highlighted.

Keywords: damping coefficient, effective damping, hysteretic energy, buckling-restrained braces.

1. Introduction

Where the response-spectrum procedure or equivalent lateral force procedure are used to analyze a structure with a damping system, response of the structure shall be modified for the effects of the system incorporated. For example, the American standard [1] modify the seismic response coefficient and design earthquake roof displacement by the damping coefficient B. In single degree of freedom system (SDFS), this coefficient is obtained according to Eq. (1).

$$B = \frac{D(T, \beta = 5\%)}{D(T, \beta)} \quad (1)$$

Where: $D(T, \beta = 5\%)$: displacement in a single degree of freedom system (SDFS), with rate of damping of 5%, T = the natural period of vibration of the system; and $D(T, \beta)$: displacement in a SDFS, with rate of damping different from 5%.

In the American standard [1], values of the damping coefficient B are given in function of the effective damping β, which is calculated according to Ec. (2).

$$\beta = \beta_I + \beta_V \sqrt{\mu} + \beta_H \quad (2)$$

Where: β_I = component of effective damping of the structure by elements of the structure, at or just below the effective yield displacement of the seismic force-resisting system due to the inherent dissipation of energy; β_V = component of effective damping due to viscous dissipation of energy by the damping system; β_H = component of effective damping of the structure due to post-yield hysteretic behavior of the seismic force-resisting system and elements of the damping system, at effective ductility demand μ.

But the type of earthquake ground motions that a structure could suffer, are not specified in this standard. Several authors have studied this problem [2, 3, 4, 5, 6, 7]. It is indicated in [2], for example, that the current damping coefficient B used in the Taiwan code would lead to very conservative estimation of the design displacement of isolation systems. Also the author shows that the damping coefficient B, derived from the earthquakes recorded in the USA, are not appropriate for use in Taiwan. A comprehensive study of the damping coefficient B for Chilean earthquake is presented in [3]. According to this bibliography, and further studies are needed.

Therefore, the objective of this paper is to study the damping coefficient B, the effective damping β, and the energy dissipated in a structure with and without BRB, subject to different kinds of earthquakes. The study is carried out on a symmetric 4-story steel moment-resisting frame that was tested without BRB at the E-Defense laboratory in Japan. The dynamic response of such unbraced bare frame was numerically simulated, obtaining a satisfactory agreement. The same numerical model was used to describe the dynamic behavior of the steel frame equipped with BRB. The inputs were three types of seismic records: near-field and far-field (intra-plate and inter-plate), with ten ground motion records in each series. These records were also scaled to match a spectrum in the Argentinian code. The hysteretic energy dissipated in the BRB was obtained for each kind of records; then, the effective damping was calculated according to the American code. Finally, the damping coefficient was calculated and discussed. The main results of each parameter studied in this paper are summarized in the conclusion.

2. Considered steel frame

2.1 Tested Bare Frame

The tested steel frame is described in the published papers [8, 9]; only a brief explanation is presented here. The specimen, shown in Fig. (1), consists of a two-bay four-story moment-resisting steel frame without any structural bracing. The two span-lengths in the main direction are 5 m while in the transversal direction the span length is 6 m; the first floor is 3.875 m high and the height of the upper floors is 3.5 m.

Fig. 1 – Steel frame tested at E-Defense.

2.2 Description of the E-Defense experiments

The experiments consisted of shaking the specimen frame with three 3-D scaled versions of a ground motion recorded in Takatori during the 1995 Kobe earthquake. The first, second and third records were scaled at 40%, 60% and 100%, respectively. The 40% record was aimed to generate only elastic deformations in the frame, the 60% record was intended to inelastic deformations and almost collapsed the frame, and the 100% record was intended to collapse of the frame.

2.3 BRB considered

The BRBs were designed according to the published papers [11]. In all cases, the steel yielding point was 230 MPa and the modulus of elasticity E was 200000 MPa. The BRB's axial stiffness K_{BRB} and the yield strength Fy_{BRB} are shown in Table 1.

Table 1 – BRB's parameters in the computational model

Floor	K_{BRB} [kN/mm]	Fy_{BRB} [kN]
4	20	151
3	32	238
2	36	277
1	41	309

Concentric diagonal braces were incorporated to the front and rear longitudinal façades, as depicted in Fig. (2). Since there are only records in the longitudinal direction, and the frame is symmetric, no braces were installed in the transverse direction.

3. Numerical modeling of the steel frame

3.1 Numerical model of the steel frame with BRB

The analysis has been carried out using a commercial software. The model consists of frame elements for columns and beams and inelastic spring elements for BRB. The parameters used in the structural modeling of the frame were obtained from [9]. Plastic hinges were considered at the ends of beams and columns, with yield moment 363 kNm; yield rotation 0.015 rad; and ultimate rotation 0.13 rad (values according to [9]).

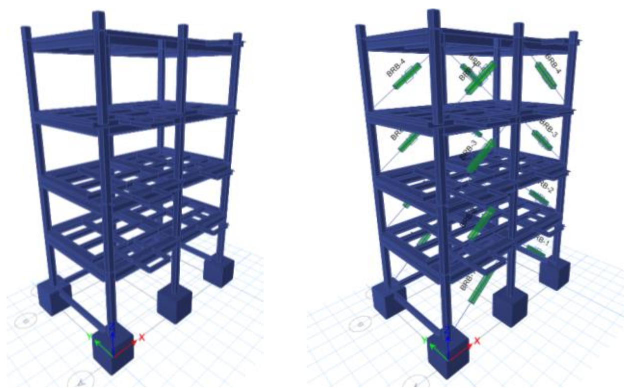

(Without BRB) (With BRB)

Fig. 2 – Numerical model of the steel frame with and without BRB.

3.3 Considered seismic records

Three kind of earthquake ground motions were considered: Near-Field and Far-Field (intra-plate and inter-plate). Ten Near-Field records (with pulse), and ten Far-Field (intra-plate) were selected from [12]; the appendix A of that document proposes ground motion record sets for collapse assessment of building structures. Other ten Far-Field (inter-plate) were also selected.

The considered records were individually scaled; the scaling factors were determined so that the resulting spectral ordinates match those of the design spectra for the city of Mendoza, Argentina for soil D, damping 5% and risk category IV. The scaling has been established for the fundamental period of the bare frame, following the recommendations of [1]. Tables 2 presents the most relevant information of these records. Analogously, Fig. (3) displays the pseudo-acceleration response spectra of the scaled and non-scaled records.

Table 2 (a) – Near-Field records

No.	Earthquake	Date	Mw	Station	Comp.	PGA [g]	PGV [cm/s]
1	Cape Mendocino	04/25/92	7.0	Petrolia	0º	0.590	48.14
2	Cape Mendocino	04/25/92	7.0	Petrolia	90º	0.662	89.68
3	Chi Chi	09/20/99	7.6	Chi Chi	N-S	0.603	78.82
4	Chi Chi	09/20/99	7.6	Chi Chi	E-W	0.814	126.22
5	Imperial Valley	10/15/79	6.5	El Centro	140º	0.410	64.86
6	Imperial Valley	10/15/79	6.5	El Centro	230º	0.439	109.82

7	Northridge	01/17/94	6.7	Sylmar-Hospital	90º	0.604	78.10
8	Northridge	17/01/94	6.7	Sylmar-Hospital	360º	0.843	129.37
9	Erzikan	03/13/92	6.7	Erzikan	N-S	0.515	83.96
10	Erzikan	03/13/92	6.7	Erzikan	E-W	0.496	64.28

Table 2 (b) – Far-Field (intra-plate) records

No.	**Earthquake**	**Date**	**Mw**	**Station**	**Comp.**	**PGA [g]**	**PGV [cm/s]**
1	Cape Mendocino	04/25/92	7.0	Rio Dell Overpass	270º	0.385	43.8
2	Cape Mendocino	04/25/92	7.0	Rio Dell Overpass	360º	0.549	41.87
3	Chi Chi	09/20/99	7.6	CHY 101	N-S	0.440	115.03
4	Chi Chi	09/20/99	7.6	CHY 101	E-W	0.535	70.65
5	Kobe	01/16/95	6.9	Nishi Akashi	0º	0.509	37.28
6	Kobe	01/16/95	6.9	Nishi Akashi	90º	0.503	36.62
7	Northridge	01/17/94	6.7	Canyon Country	0º	0.410	42.97
8	Northridge	01/17/94	6.7	Canyon Country	270º	0.482	44.91
9	Duzce	11/12/99	7.1	Bolu	0º	0.728	56.44
10	Duzce	11/12/99	7.1	Bolu	90º	0.822	62.10

Table 2 (c) – Far-Field (inter-plate) records

No.	**Earthquake**	**Date**	**Mw**	**Station**	**Comp.**	**PGA [g]**	**PGV [cm/s]**
1	Pisco (Perú)	15/08/07	8.0	La Molina	E-W	0.08	11.64
2	Pisco (Perú)	15/08/07	8.0	La Molina	N-S	0.07	159.3
3	Maule (Chile)	08/04/10	8.8	Maule	Ch. 1	0.401	69.28
4	Maule (Chile)	08/04/10	8.8	Maule	Ch. 2	0.286	52.58
5	México	19/09/85	8.0	CDAF	N90W	0.096	37.74
6	México	19/09/85	8.0	CDAO	N00E	0.07	35.98
7	México	19/09/85	8.0	CU01	S00E	0.029	10.16
8	México	19/09/85	8.0	CU01	N90W	0.034	9.27
9	Tohoku (Japan)	11/03/11	9.0	MYG004	E-W	1.24	4798

10	Tohoku (Japan)	11/03/11	9.0	MYG004	N-S	2.58	5808

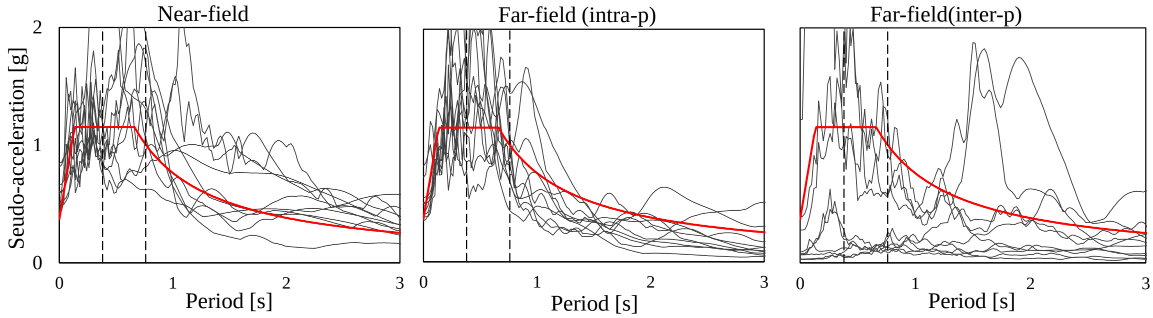

Fig. 3 (a) – Absolute pseudo-acceleration response spectra (non-scaled records)

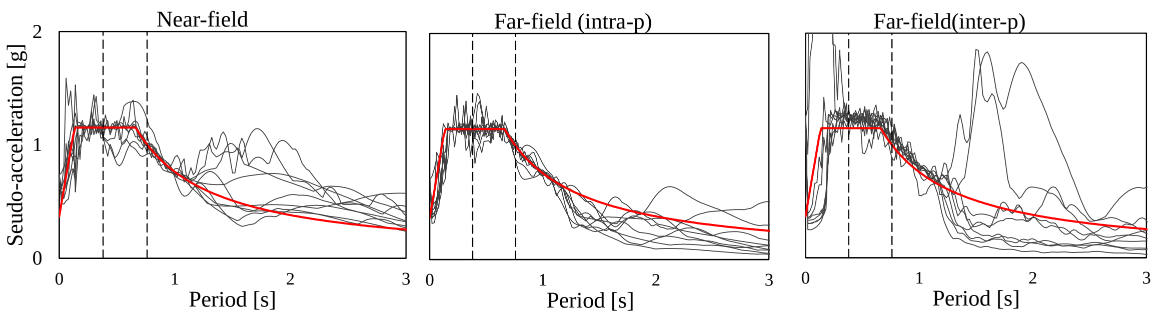

Fig. 3 (b) – Absolute pseudo-acceleration response spectra (scaled records)

4. Numerical results and discussion

Results of the analysis that are presented in this section include: energy dissipated, the effective damping β, and the damping coefficient B, obtained in the E-Defense's frame, with and without BRB. The frame was subject to the 30 records described in previous section (scaled and non-scaled). Also, the damping coefficient B in a SDFS is studied.

4.1 Energy dissipated

The total hysteretic energy dissipated in the BRB was considered for the BRB frame; and the energy dissipated in plastic zones was evaluated in the bare frame.

Fig. 4 shows that energy referred to the input, and ordered according to increasing PGA (peak ground acceleration).

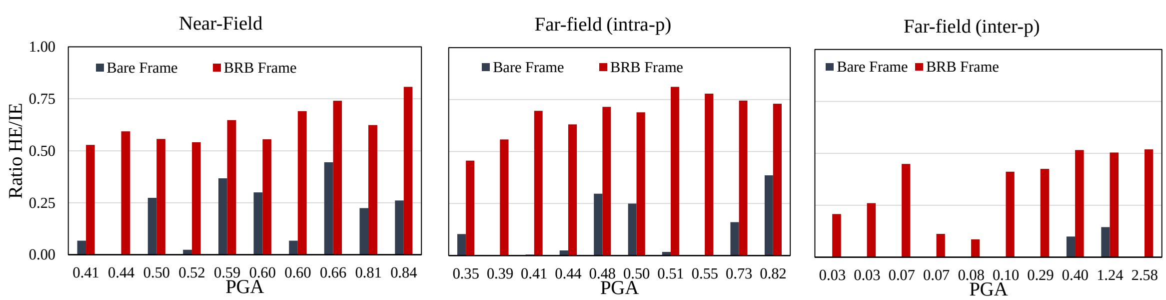

Fig. 4 (a) – Hysteretic energy/input energy (HE/IE) vs. PGA (non-scaled records).

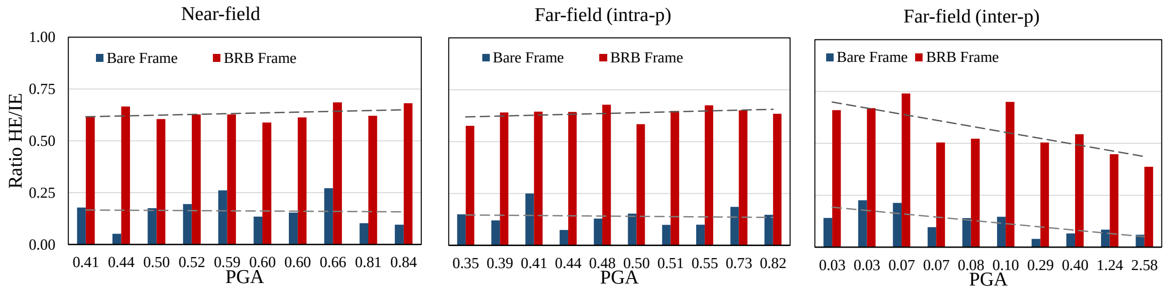

Fig. 4 (b) – Hysteretic energy/input energy (HE/IE) vs. PGA (scaled records).

In all cases analyzed, the ratio hysteretic energy/input energy is much higher in BRB frame. For Near-Field and Far-Field (intra-plate) scaled records, in bare frame and BRB frame, this ratio does not present significant variations with respect to PGA.

4.2 Effective damping β

The effective damping β was calculated by Eq. (2). In this equation, the inherent dissipation of energy β_I was adopted according to the damping value considered in the calibration of the numerical model of the bare frame (β_I = 0.025). The effective damping due to viscous dissipation of energy β_V was null. And the hysteretic damping β_H is expressed by Eq. (3), [1].

$$\beta_H = q_H \left(0.64 - \beta_I\right)\left(1 - \frac{1}{\mu}\right) \tag{3}$$

The hysteresis loop adjustment factor q_H, was determined by Eq. (4), [1].

$$q_H = 0.67\,\frac{T_S}{T_1} \tag{4}$$

Where: T_S = 0.66 s, period defined by the ratio (SD1 / SDS) = (0.76 / 1.15) in the Argentinian code; and T_1 = 0.40 s, period of the fundamental mode of vibration of the structure with BPB. It was obtained q_H = 1.1, but q_H = 1.0 is adopted, after the upper limit gave for [1].

The effective ductility demand μ was determined by Eq. (5), [1].

$$\mu = \frac{D_{1D}}{D_Y} \tag{5}$$

Where: D_{1D} is the roof displacement due to the design earthquake ground motion; and D_Y is the roof displacement at the effective yield point of the seismic force-resisting system [1]. In this paper: D_{1D} was obtained from each records, by nonlinear time history analysis; and D_Y was calculated according to the first plastic zone appeared in the structure with and without BRB (these displacements were determined by a nonlinear static analysis).

Figure 5 shows the effective damping β in the structure, obtained according to Eq. (2). The bare frame and the BRB frame were considered, subject to scaled and non-scaled records. The mean value of the effective damping β for scaled records are shown in Table 3, ordered according to increasing PGA.

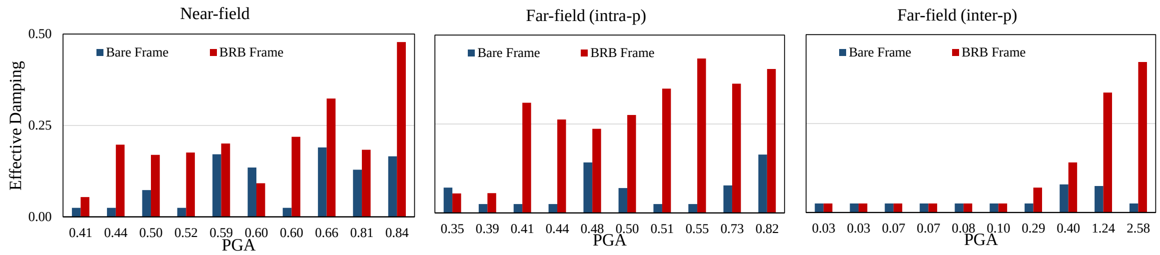

Fig. 5 (a) – Effective damping β vs. PGA (non-scaled records)

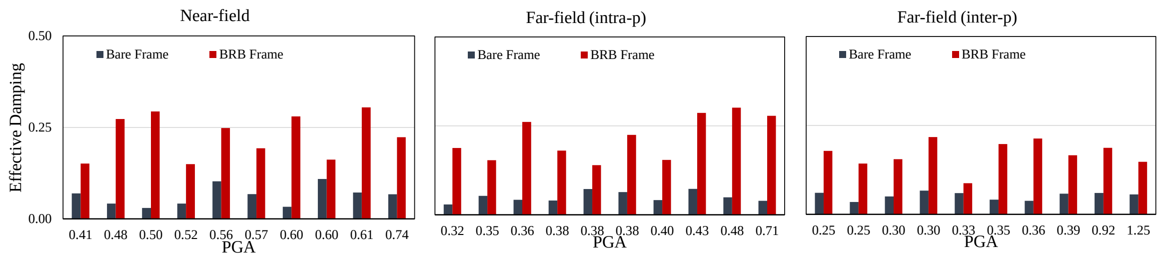

Fig. 5 (b) – Effective damping β vs. PGA (scaled records)

Table 3 – Effective damping β [%] (mean values for scaled records)

Item	**Scaled record**		
	Near-Field	Far-Field (intra-plate)	Far-Field (inter-plate)
BRB frame	22.8	21.7	16.9
Bare frame	6.4	5.0	5.3

For scaled records, the effective damping β does not present significant variations with respect to PGA. Its value is about 20 % for BRB frame and 5% for Bare frame; these values are slightly lower for Far-Field, inter-plate.

4.3 Damping Coefficient B

The damping coefficient B, defined in Ec. (1), is studied in this section. This coefficient is analized according to: [1], E-Defense frame with and without BRB, and in a SDFS.

4.3.1 Damping coefficient B in [1]

Damping coefficient B are given in [1] for values of the effective damping β; this function is shows in Fig. 6.

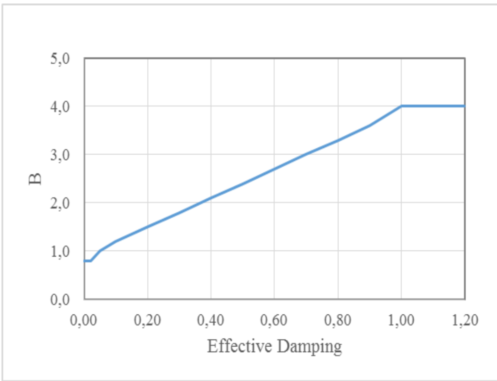

Fig. 6 – Damping coefficient B vs. effective damping β (according to [1])

4.3.2. Damping coefficient B in E-Defense frame

The damping coefficient B was obtained in the E-Defense's frame, with and without BRB, subject to the 30 scaled and non-scaled records. For each record, the effective damping β was considered, according to the previous section. With these β values, the damping coefficient B was obtained according to [1]. Fig. 7 shows the mean values of the B for scaled and non-scaled records.

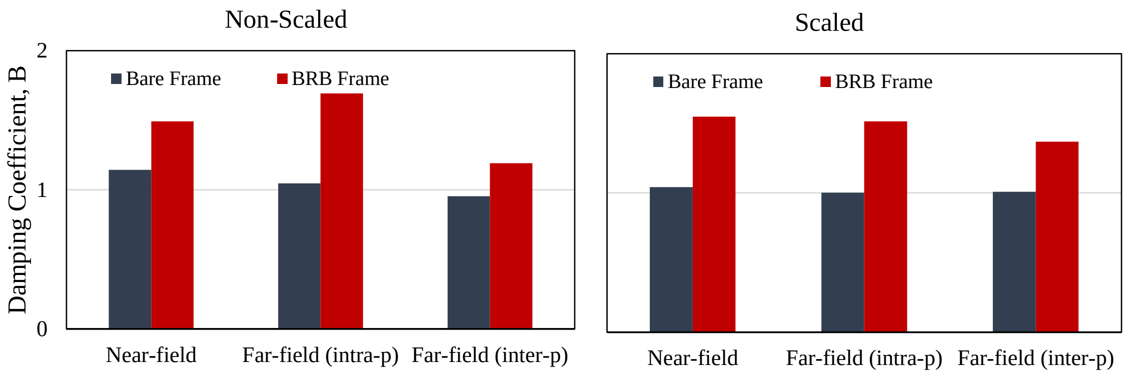

Fig. 7 – Damping Coefficient B in E-Defense's frame (mean values)

For scaled records, the damping coefficient B does not present significant variations with respect to the kind of records considered. The mean value is about 1.5 for BRB frame and 1.0 for Bare frame (and slightly lower for Far-Field, inter-plate).

4.3.3. Damping coefficient B in a SDFS.

In this section, the damping coefficient B is calculated in a SDFS according to Ec. (1). The effective damping considered were β = 2.5, 5, 10, 20, 30 and 50 %. Displacement spectrum were obtained for each β, such as shown in Fig. 8 for Near-Field records. Then, damping coefficient B is calculated dividing each ordinate of the displacement spectrum with β = 5 % with respect to ordinate of the displacement spectrum (with different β), according to Ec. (1). The damping coefficient B as a function of the period are shown in Fig. 9. The damping coefficient B for each effective damping β according to [1], also is drawn in dashed line in this Figure.

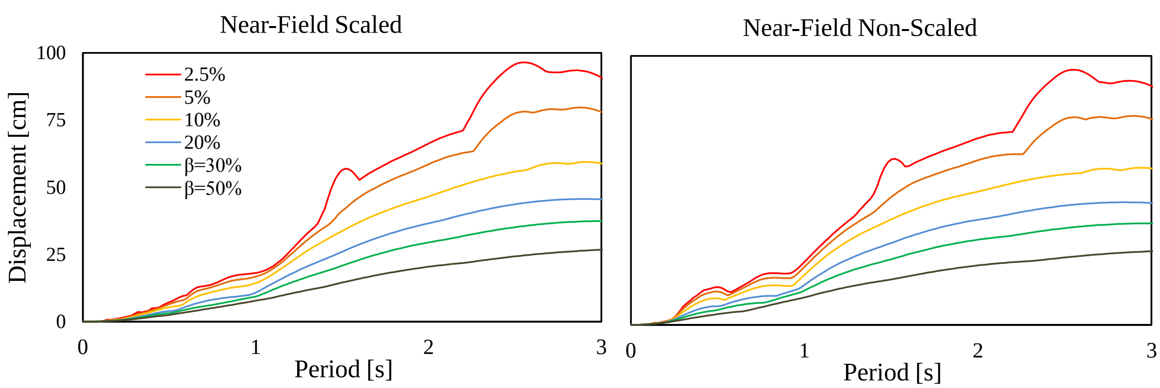

Fig. 8 – Displacement spectrum for Near-Field records.

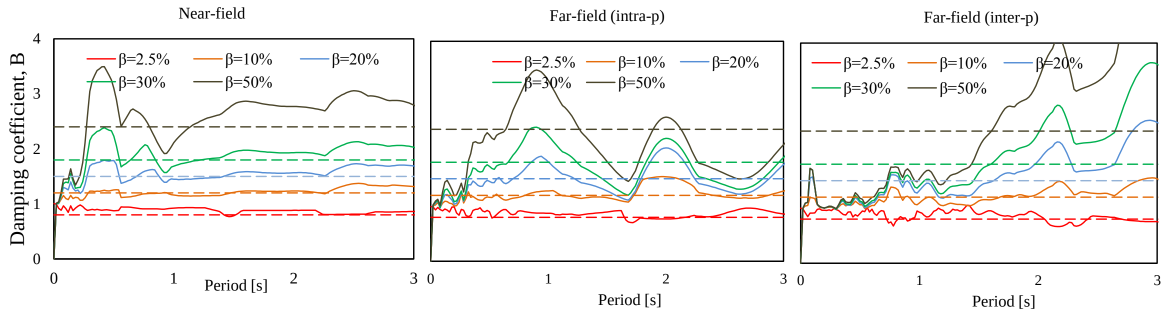

Dashed line: B for different β, according to [1]

Fig. 9 (a) – Damping Coefficient B in a SDFS (non-scaled records).

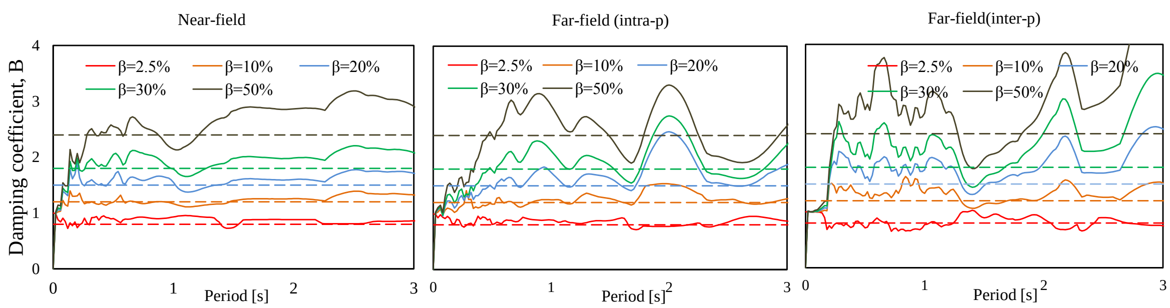

Dashed line: B for different β, according to [1]

Fig. 9 (b) – Damping Coefficient B in a SDFS (scaled records).

For scaled records, in general, the damping coefficient B obtained is upper that the value indicated by the American code [1]. For high values of effective damping β, and in certain interval of periods (specially for Far-Field, inter-plate), the above statement is not met. In the case of non-scaled records, in certain intervals of T (specially for Far-Field, inter and intra-plate), the B obtained is below that the value indicated in [1].

Finally, Figure 10 presents the variation of the damping coefficient B with the effective damping β (only for scaled records), in a SDFS with a period according to the bare frame. In this case, the damping coefficient B is calculated with the methodology here descripted. Also, the damping coefficient B obtained with [1] are considered.

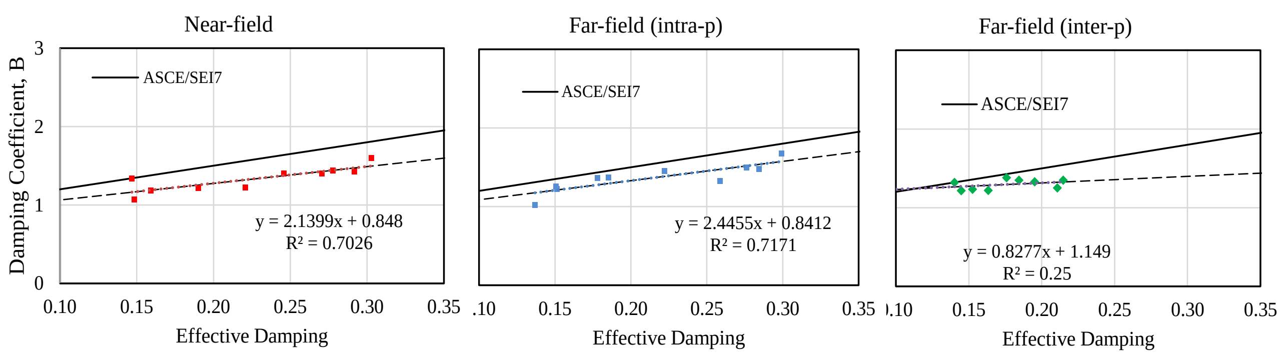

Fig. 10 – Damping Coefficient B vs. effective damping β (scaled records).

For Near-Field and Far-Field (intra-plate) records, the trend line of the variations B vs. β is close to [1]. But for Far-Field (inter-plate) records the difference is greater.

5. Conclusion

This paper analyzes energy dissipated, effective damping, and damping coefficient in a frame with and without BRB.

The frame, modeled with a commercial computer program, was subject to three kinds of earthquake ground motions: 10 Near-Field records and 20 Far-Field records (10 intra-plate and 10 inter-plate). The response of the structure was obtained for scaled and non-scaled records. Scaling was performed according to a spectrum of Argentine code.

From this study, the following results are highlighted:

. Energy dissipated: Braces in BRB frame dissipate much more energy than plastic zones in bare frame. Only Near-Field and Far-Field (intra-plate) scaled records reached a ratio “hysteretic energy / input energy” approximately constant.

. Effective damping β: The bare frame had an effective damping β equal to 5% (mean value), and up to 20% when the frame incorporates BRB (structures subject to scaled records). No correlation was found between effective damping β and the PGA.

. Damping coefficient B:

.. E-Defense frame subject to scaled records: The mean value of B was 1.0 for bare frame, and 1.5 for BRB frame (with values a little smaller for Far-Field, inter-plate).

.. For the records scaled considered in this study, the damping coefficient B in a SDFS, is generally upper than the value recommended by the American code [1], except for certain values of period in Far-Field (inter-plate).

.. For the Far-Field (inter-plate) scaled records, in a SDFS con period according to bare frame, the variation of the damping coefficient B with the effective damping β does not appear to follow the trend indicated in [1].

With all the parameters analyzed, important variations were obtained in the case of non-scaled records.

Further studies are needed to better specify the damping coefficient B to be used with different records, especially with Far-Field (inter-plate) records.

5. References

[1] ASCE/SEI 7 (2010): Minimum design loads for buildings and other structures. *American Society of Civil Engineers*.

[2] Yu-Yuan Lin (2006): Statistical study on damping modification factors adopted in Taiwan’s seismic isolation design code by using the 21 September 1999 Chi-Chi earthquake, Taiwan. *Engineering Structures*, **29** (2007) 682–693.

[3] Sáez Uribe, A (2014): Evaluación del método de análisis modal espectral para edificios con sistemas pasivos de disipación de energía utilizando registros sísmicos chilenos. Tesis de Maestría. Universidad de Chile.

[4] Neaz Sheikh M., Hing-Ho Tsang, Yaghmaei-Sabegh S, Anbazhagan P (2013): Evaluation of damping modification factors for seismic response spectra. In S. Anderson (Eds.), *Australian Earthquake Engineering Society Conference* 2013 (pp. 1-13). Tasmania: Australian Earthquake Engineering Society.

[5] Kyung-Won M, Kim J, Hwang J (2004). Evaluation of equivalent damping ratio of a structure with added dampers. *Engineering Structures*, **26** (2004) 335–346.

[6] Borzi B and Elnashai A (2000): Refined force reduction factors for seismic design. *Engineering Structures* **22** (2000) 1244–1260.

[7] Mollaioli F, Liberatore L, and Lucchini A (2015): Authors’ reply to discussion by G.P. Mavroeidis of ‘‘Displacement Damping Modification Factors for pulse-like and ordinary records”. *Engineering Structures*, **100** (2015) 779–781.

[8] Tada M, Ohsaki M, Yamada S, Motoyui S, and Kasai K (2007): E-defense test on full-scale steel buildings: part 3-analytical simulation of collapse. NEES/E-Defense collaborative research program on steel structures.

[9] Pavan A. (2008): Blind prediction of a full-scale 3d steel frame tested under dynamic conditions. MSc Dissertation, Centre for Post - Graduate Training and Research in Earthquake Engineering and Engineering Seismology (ROSE School), Pavia, Italy.

[10] Aguiar R (2004): Espectros sísmicos de riesgo uniforme para verificar desempeño estructural en paises sudamericanos. Boletín Técnico, Versión impresa ISSN 0376-723X, IMME v.42 n.1 Caracas.

[11] Palazzo G, Martín P, Calderón F, Roldán V and López Almansa F (2015): Numerical study of the seismic efficiency of buckling-restrained braces for near and far-fault inputs. *The Open Civil Engineering Journal*, **9**, (Suppl. 1, M 7) 281-294.

[12] FEMA P695 (2009): Quantification of building seismic performance factors. Federal Emergency Management Agency.